Gangliosides Link the Acidic Sphingomyelinase–Mediated Induction of Ceramide to 12-Lipoxygenase–Dependent Apoptosis of Neuroblastoma in Response to Fenretinide

Penny E. Lovat, Federica Di Sano, Marco Corazzari, Barbara Fazi, Raffaele Perrone Donnorso, Andy D. J. Pearson, Andrew G. Hall, Christopher P. F. Redfern, Mauro Piacentini

Background: **The lipid second messenger ceramide, which is generated by acidic and neutral sphingomyelinases or ceramide synthases, is a common intermediate of many apoptotic pathways. Metabolism of ceramide involves several enzymes, including glucosylceramide synthase and GD3 synthase, and results in the formation of gangliosides (GM3, GD3, and GT3), which in turn promote the generation of reactive oxygen species (ROS) and apoptosis. Fenretinide, a retinoic acid derivative, is thought to induce apoptosis via increases in ceramide levels, but the link between ceramide and subsequent apoptosis in neuroblastoma cells is unclear.** ***Methods:*** **SH-SY5Y and HTLA230 neuroblastoma cells were treated with fenretinide in the presence or absence of inhibitors of enzymes important in ceramide metabolism (fumonisin B_1, inhibitor of ceramide synthase; desipramine, inhibitor of acidic and neutral sphingomyelinases; and PDMP, inhibitor of glucosylceramide). Small interfering RNAs were used to specifically block acidic sphingomyelinase or GD3 synthase activities. Apoptosis, ROS, and GD3 expression were measured by flow cytometry.** ***Results:*** **In neuroblastoma cells, ROS generation and apoptosis were associated with fenretinide-induced increased levels of ceramide, glucosylceramide synthase activity, GD3 synthase activity, and GD3. Fenretinide also induced increased levels of GD2, a ganglioside derived from GD3. Inhibition of acidic sphingomyelinase but not of neutral sphingomyelinase or ceramide synthase, blocked fenretinide-induced increases in ceramide, ROS, and apoptosis. Exogenous GD3 induced ROS and apoptosis in SH-SY5Y cells but not in SH-SY5Y cells treated with baicalein, a specific 12-lipoxygenase inhibitor. Exogenous GD2 did not induce apoptosis.** ***Conclusions:*** **A novel pathway of fenretinide-induced apoptosis is mediated by acidic sphingomyelinase, glucosylceramide synthase, and GD3 synthase, which may represent targets for future drug development. GD3 may be a key signaling intermediate leading to apoptosis via the activation of 12-lipoxygenase. [J Natl Cancer Inst 2004;96:1288–99]**

Neuroblastoma is the most common extracranial solid tumor of childhood *(1)*, and high-risk disease is usually treated with chemotherapy and autologous bone marrow transplantation. The biologic behavior of neuroblastoma is variable and the disease can resolve spontaneously, suggesting that advances in treatment may come from a greater understanding of neuroblastoma cell biology and of methods to increase the targeting of conventional therapy. The most substantial advance in treatment in recent years has come from the inclusion of 13-*cis* retinoic acid as a biologic therapy targeting minimal residual disease *(2)*, but further refinements of retinoic acid therapy are limited by the fact that retinoic acid can induce differentiation of neuroblastoma cells, rendering them resistant to chemotherapy *(3)*. However, some synthetic derivatives of retinoic acid, such as fenretinide (N-[4-hydroxyphenyl]retinamide), can induce apoptosis rather than differentiation *(4,5)* and, unlike 13-*cis* retinoic acid, show synergistic responses with chemotherapeutic drugs *in vitro (6,7)*. Because fenretinide is well tolerated, there is substantial interest in using fenretinide for clinical trials in neuroblastoma and other cancers [for examples, see *(8,9)*]. Fenretinide is also a valuable tool for defining apoptotic signaling pathways and for defining mechanisms of synergy with chemotherapeutic drugs. Increasing the specificity of chemotherapy agents through targeting cell-specific synergistic responses may provide more effective and less toxic treatment than is possible with conventional chemotherapeutic drugs.

In neuroblastoma cells, fenretinide-induced apoptosis involves mitochondria and is caspase-dependent *(10)*. Retinoic acid receptor (RAR) antagonists and antioxidants inhibit fenretinide-induced apoptosis, suggesting that signaling pathways involving RARs and reactive oxygen species (ROS) are both required for fenretinide-induced apoptosis *(10)*. However, the ability of fenretinide to induce ROS may be the key to its apoptosis-inducing properties. Recent studies *(11,12)* have shown that, in two neuroblastoma cell lines, oxidative stress induced by fenretinide is mediated by 12-lipoxygenase activity.

Affiliations of authors: Northern Institute for Cancer Research, University of Newcastle upon Tyne, Newcastle upon Tyne, U.K. (PEL, ADJP, AGH, CPFR); Department of Biology, University of Rome, Rome, Italy (FDS, BF, MP); Istituto Nazionale Malattie Infettive–Istituto di Ricovero e Cura a Carattere Scientifico Lazzaro Spallanzani, Rome (MC, MP); The 'Regina Elena' National Cancer Institute, Rome (RPD).

Correspondence to: Chris P. F. Redfern, PhD, Northern Institute for Cancer Research, University of Newcastle upon Tyne, Newcastle upon Tyne, NE2 4HH, U.K. (e-mail: chris.redfern@ncl.ac.uk).

See "Notes" following "References."

DOI: 10.1093/jnci/djh254

Journal of the National Cancer Institute, Vol. 96, No. 17,

Sustained induction of the growth and DNA damage (GADD)-inducible transcription factor GADD153 *(11)* is a consequence of increased ROS *(11),* and subsequent induction of the pro-apoptotic protein Bak *(13)* accompanies mitochondrial cytochrome c release and caspase-3-dependent apoptosis *(10).*

In addition to its effects on ROS, fenretinide has been reported to increase intracellular levels of the lipid secondary messenger ceramide in tumor cells *(5,14–16).* At high concentration, fenretinide appears to increase ceramide levels in some human neuroblastomas, prostate cancers, leukemias, and endothelial cells through a *de novo* synthesis pathway by activating the rate-limiting enzyme serine palmitoyltransferase *(14–17).* Paradoxically, fumonisin B_1, an inhibitor of ceramide synthase, does not inhibit fenretinide-induced apoptosis of neuroblastoma cells *(14).* High concentrations of fenretinide can induce necrosis as well as apoptosis *(5);* therefore, it is possible that more subtle apoptotic effects are mediated by mechanisms that increase ceramide levels by means other than *de novo* synthesis. One such mechanism is membrane sphingomyelin hydrolysis by sphingomyelinases *(18,19)* (Fig. 1). Both neutral and acidic sphingomyelinases, the two major classes of this enzyme, are important in ceramide generation and apoptosis *(20–24).*

In addition to uncertainty about the mechanisms by which ceramide is generated in neuroblastoma cells in response to fenretinide treatment, the fate of increased ceramide and the role of ceramide metabolites in apoptotic signaling in response to fenretinide are not known. The aim of this study was to test the hypothesis that sphingomyelinases are involved in fenretinide-induced apoptosis of neuroblastoma cells and to use chemical inhibitors and RNA interference to identify the downstream elements of ceramide signaling.

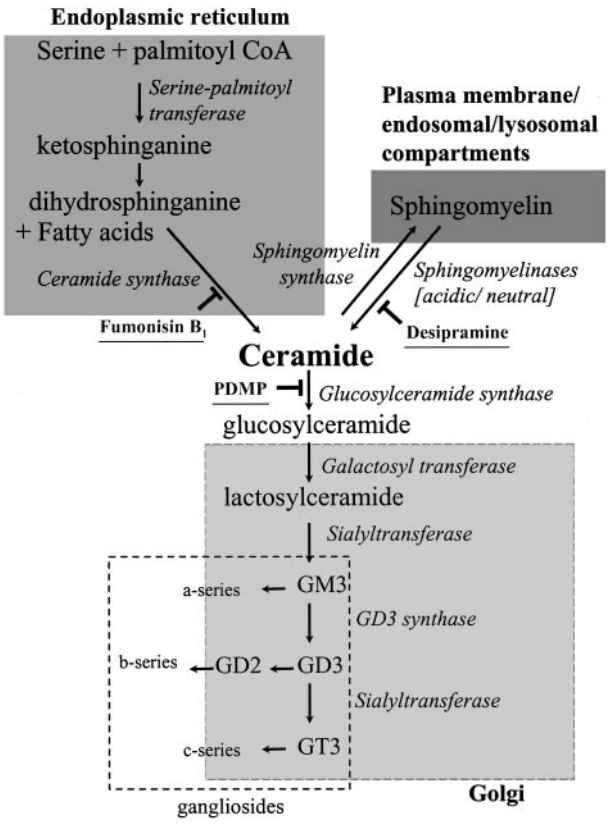

Fig. 1. Biochemical pathways of ceramide generation and metabolism. Main enzymes are shown in **italics**, and inhibitors are **underlined**. Ceramide is derived from two main pathways operating in different cellular compartments: hydrolysis of membrane-derived sphingomyelin and *de novo* synthesis from serine and palmitoyl CoA. It is subsequently metabolized to gangliosides of the a-, b-, and c-series, which include GD3 and GD2.

METHODS

Cell Culture and Treatment With Fenretinide, Enzyme Inhibitors, and Exogenous Gangliosides

The human neuroblastoma cell lines SH-SY5Y (MYCN not amplified) *(25)* and HTLA230 (MYCN amplified) *(12)* were grown in complete culture medium consisting of a 1:1 mixture of Dulbecco's Modified Eagle Medium and Ham's F12 (Life Technologies, Paisley, U.K.) supplemented with 10% fetal bovine serum (Life Technologies) and grown in a humidified atmosphere of 5% CO_2 in air.

For all experiments, cells were seeded into tissue culture flasks and allowed to attach for 24 hours (HTLA230 cells) or 48 hours (SH-SY5Y cells) before treatment. The seeding density varied according to the type of experiment; for flow cytometry and RNA interference experiments to measure apoptosis and ROS generation, 1×10^6 cells were seeded into 25-cm^2 flasks (Costar, High Wycombe, U.K.) in 8 mL of culture medium. For immunofluorescence experiments, 2×10^6 cells were seeded into 25-cm^2 flasks in 8 mL of culture medium.

Ethanol was the diluent for fenretinide (Janssen-Cilag, Basserdorf, Switzerland) and for the disialogangliosides Neu5Acα8Neu5Acα3Galβ4GlcCer (GD3) and GalNAcβ4 (Neu5Acα8Neu5Acα3)Galβ4GlcCer (GD2) (both from Calbiochem, San Diego, CA). Control cells were treated with a volume of ethanol (less than 0.1% of the final culture volume) equivalent to that used for fenretinide, GD3, or GD2. Fumonisin B_1, a specific inhibitor of ceramide synthase (final concentration = 20 μ*M;* Sigma Chemical, Poole, U.K.), was diluted in ethanol. Desipramine hydrochloride, a broad-spectrum inhibitor of sphingomyelinase (final concentration = 5 μ*M;* Sigma), neutral sphingomyelinase spiroepoxide inhibitor (final concentration = 1 μ*M;* Alexis Biochemicals, San Diego, CA), and 1-phenyl-2-decanoylamino-3-morpholino-1-propanol (PDMP, an inhibitor of glucosylceramide synthase; final concentration = 10–30 μ*M;* Sigma) were diluted in dimethyl sulfoxide. For experiments involving inhibitors, cells were treated with the inhibitor or control diluent for 1 hour and then treated with fenretinide for 24 hours. Unless stated otherwise, the concentration of fenretinide used was 3 μ*M.* For experiments involving baicalein (final concentration = 1 μ*M,* a specific inhibitor of 12-lipoxygenase at this concentration, diluted in ethanol), cells were treated for 2 hours and then treated with fenretinide, GD3, or GD2, as previously described *(11).*

Flow Cytometry

Flow cytometry was used to evaluate apoptosis, ROS generation, and endogenous GD3 and GD2 levels. Apoptosis was evaluated by staining cells with propidium iodide (100 μg/mL final concentration), as previously described *(10).* ROS generation was evaluated by staining cells with 10 μ*M* 5- (and 6-)chloromethyl-2′,7′-dihydrodichlorofluorescein diacetate (CMH_2DCFA) for 20 minutes at 37 °C in the dark, as previously described *(10,11).* Endogenous GD3 and GD2

were detected by immunofluorescence flow cytometry; cells were detached with trypsin, washed with phosphate-buffered saline (PBS), and fixed in 4% paraformaldehyde in PBS for 10 minutes at room temperature. The cells were permeabilized in a buffer containing 0.5% Triton X-100 for 2 minutes at room temperature and stained with 200 μL of a mouse monoclonal anti-GD3 antibody (Calbiochem, diluted 1:100) or with a mouse anti-GD2 antibody (mouse immunoglobulin G2 [IgG2a], diluted to 1 μg/mL; a kind gift from Dr. Holger N. Lode, Charite Universitatsmedizin, Berlin, Germany) for 1 hour at room temperature. Primary antibodies were diluted in PBS containing 5% bovine serum albumin, and were detected with 10 μg of a secondary goat anti-mouse IgG antibody conjugated with fluorescein isothiocyanate (Molecular Probes, Leiden, The Netherlands, for detection of GD3; Sigma for detection of GD2) diluted in PBS containing 5% bovine serum albumin in a final volume of 200 μL. For each sample, 20 000 events were acquired for flow cytometry, as previously described *(11)*. Control samples stained with secondary antibody alone were included in each experiment.

RNA Interference of Acidic Sphingomyelinase and GD3 Synthase

The Ambion Silencer small interfering RNA (siRNA) construction kit (product 1620, Ambion Europe, Huntingdon, U.K.) was used to generate double-stranded small interfering RNAs (ds-siRNAs) according to the manufacturer's instructions. The targets (Table 1) were designed using the Ambion online resource (www.ambion.com/techlib/misc/siRNA_finder.html), and primer oligonucleotides were obtained from TAGN (Newcastle, U.K.). Pre-validated glyceraldehyde-3-phosphate dehydrogenase (GAPDH)-specific sense and antisense templates provided with the Ambion Silencer kits were used to generate a control ds-siRNA unrelated to the target mRNA to control for nonspecific effects of the gene knockdown process. Each ds-siRNA (final concentration = 5 n*M*) was transiently transfected into 1×10^6 SH-SY5Y cells by using Lipofectamine 2000 (Life Technologies) for 24 hours, according to the manufacturer's instructions. Fetal calf serum was added to a final concentration of 10% 6 hours after the addition of Lipofectamine and ds-siRNA. After 24 hours, the medium was replaced with an equal volume of complete culture medium containing 5 μ*M* fenretinide or the appropriate volume of ethanol (control vehicle) for 6–24 hours. Cells were subsequently harvested with trypsin for analysis. For experiments in which ceramide or sphingomyelin levels were measured after RNA interference, the medium was replaced after the 24-hour transfection period with fresh medium containing 0.1% fetal calf serum, 5 μ*M* fenretinide, or ethanol control, as appropriate, and 1 μCi/mL [^{3}H]-palmitic acid (Amersham Biosciences, Chalfont St. Giles, U.K.) for 18 hours.

In preliminary experiments, two ds-siRNA targets for acidic sphingomyelinase (acid lysosomal sphingomyelin phosphodiesterase 1, EC 3.1.4.12) and three for GD3 synthase (α-*N*-acetylneuraminate α-2,8-sialyltransferase, EC 2.4.99.8) (Table 1) were screened by comparing their ability to inhibit fenretinide-induced apoptosis of SH-SY5Y cells. For the acidic sphingomyelinase ds-siRNAs, target sequence 11 (Table 1) reduced apoptosis by approximately 20%, whereas target sequence 18 reduced apoptosis by approximately 50%. Acidic sphingomyelinase target sequence 18 was therefore used for all subsequent experiments. For the GD3 synthase ds-siRNAs, all three target sequences were equally effective at reducing fenretinide-induced apoptosis to control levels; only target sequence 43 was used for subsequent experiments.

Although RNA interference produces robust silencing of targeted mRNA, off-target (i.e., nonspecific) effects can occur with sequences of 11–15 contiguous nucleotides *(26)*. From BLAST *(27)* searches of the GenBank nonredundant nucleotide sequence database for the acidic sphingomyelinase target 18 sequence, 11 and 12 contiguous nucleotides matched cAMP-specific phosphodiesterase 8B and cGMP phosphodiesterase, respectively, but there were no matches of greater length to other known phosphodiesterases. For the GD3 synthase target sequence 43, there were no contiguous sequence matches of more than nine nucleotides to known sialyltransferases other than to GD3 synthase. With respect to potential matches of the acidic sphingomyelinase (target 18) and GD3 synthase (target 43) sequences to other genes, there were no matches of more than 15 contiguous nucleotides to known transcripts. Therefore, although off-target effects cannot be discounted, the ds-siRNA probes used here were of high specificity to the selected targets.

Western Blotting

Total proteins (25 μg) were extracted from SH-SY5Y control cells, SH-SY5Y cells transfected with ds-siRNA for acid sphingomyelinase, or SH-SY5Y cells transfected with ds-siRNA for acid sphingomyelinase, treated with fenretinide for 24 hours, and separated by electrophoresis through 12.5% sodium dodecyl sulfate–polyacrylamide gel electrophoresis gels and electroblotted onto nitrocellulose membranes *(11)*. Acid sphingomyelinase was detected by incubating the membranes with a polyclonal goat anti-acid sphingomyelinase antibody (a kind gift from Pro-

Table 1. Sense and antisense oligonucleotide templates for double-stranded small interfering RNA synthesis

mRNA target	ID code	Orientation	Oligonucleotide template (5′ to 3′)*
Acidic sphingomyelinase	18	Antisense	**AATACAGCAAGTGTGACCTGC**CCTGTCTC
		Sense	**AAGCAGGTCACACTTGCTGTA**CCTGTCTC
Acidic sphingomyelinase	11	Antisense	**AAGCTGTGCAATCTGCTGAAG**CCTGTCTC
		Sense	**AACTTCAGCAGATTGCACAGC**CCTGTCTC
GD3 synthase†	7	Antisense	**AAATGGAAGACTGCTGCGACC**CCTGTCTC
		Sense	**AAGGTCGCAGCAGTCTTCCAT**CCTGTCTC
GD3 synthase	12	Antisense	**AAGAGCATGTGGTATGACGGG**CCTGTCTC
		Sense	**AACCCGTCATACCACATGCTC**CCTGTCTC
GD3 synthase	43	Antisense	**AACCCCAACTTTCTGCGTAGC**CCTGTCTC
		Sense	**AAGCTACGCAGAAAGTTGGGG**CCTGTCTC

*mRNA sequence in bold.

†GD3 synthase = α-*N*-acetylneuraminate α-2,8-sialyltransferase.

fessor Sandhoff, Department of Chemistry and Biochemistry, University of Bonn, Bonn, Germany) diluted 1:2500 in blocking solution (5% nonfat dry milk in PBS containing 0.1% vol/vol Tween 20) for 1 hour at room temperature. Antibody binding was visualized with a peroxidase-conjugated affinity-purified rabbit anti-goat IgG (Jackson Laboratories, West Grove, PA) that was diluted 1:10 000 in blocking solution and incubated with the membrane for 1 hour at room temperature; the secondary antibody was detected by enhanced chemiluminescence. β-Tubulin was detected with a monoclonal mouse anti-β-tubulin antibody (Sigma; diluted 1:1000) and a peroxidase-conjugated affinity-purified goat anti-mouse IgG (Bio-Rad, Hemel Hempstead, U.K.; diluted 1:5000) as a control for protein loading.

Measurement of Acidic Sphingomyelinase Activity

Acidic sphingomyelinase activity was assayed as described by Wiegmann et al. *(28)*. Briefly, cells were harvested by scraping, washed twice with PBS, and suspended in 200 μL of 20 m*M* HEPES buffer (pH 7.4) containing 0.2% Triton X-100, 1 m*M* phenylmethylsulfonyl fluoride, and a protease inhibitor cocktail. After incubation for 15 minutes at 4 °C, cells were homogenized by passing them through an 18-gauge needle, nuclei and debris were removed by centrifugation at 800*g*, and 50 μg of protein was subsequently incubated for 2 hours at 37 °C in a buffer containing 250 m*M* sodium acetate, 1 m*M* EDTA (pH 5.0), and 2 μL of [N-methyl-^{14}C]-sphingomyelin (specific activity, 55 mCi/mMol; Amersham Biosciences). Phosphorylcholine was then extracted with 800 μL of chloroform:methanol [2:1 (vol/vol)], and 250 μL of water. Radioactive phosphorylcholine produced from [^{14}C]-sphingomyelin was measured by liquid scintillation counting. Acidic sphingomyelinase activity was calculated as picomoles per milligram per hour, and results were expressed as a percentage of the activity in control uninduced cells.

Measurement of Glucosylceramide Synthase Activity

Glucosylceramide synthase (ceramide glucosyltransferase, EC 2.4.1.80) activity was measured as described previously *(29)*. Briefly, 1×10^6 cells in 5 mL were incubated with 5 μ*M* 6-(*N*-(7-nitrobenzen-2-oxa-1,3-diazol-4-yl)-amino)hexanoyl-sphingosine (NBD; Molecular Probes, Eugene, OR). Lipids were extracted and separated by high-performance thin-layer chromatography. Glucosylceramide–NBD was detected under UV illumination and extracted from the silica gel; fluorescence was measured with a Perkin-Elmer LS-5 luminescence spectrophotometer (Perkin-Elmer, Monza, Italy). Glucosylceramide synthase activity was then expressed relative to a standard glucosylceramide–NBD fluorescence calibration curve.

Cellular Ceramide and Sphingomyelin Content

To determine cellular ceramide and sphingomyelin content, cells were treated with [^{3}H]-palmitic acid (Amersham Biosciences) for 18 hours, as described previously *(30)*, detached with trypsin and washed twice with PBS; total cellular lipids were then extracted. The lipids were subjected to mild alkaline hydrolysis with 0.1 *M* methanolic KOH for 1 hour at 37 °C and re-extracted with chloroform. The chloroform phase was then analyzed by thin-layer chromatography using different solvent systems for ceramide and sphingomyelin *(16)*. Lipids were visualized by incubating the plates in 3% cupric acetate in 8% phosphoric acid and then heating them in an oven for 15 minutes at 180 °C, according to Spinedi et al. *(30)*. Tritium in the thin-layer chromatography–resolved lipid band and total tritium in equal aliquots of the extracted lipids were quantified by liquid scintillation counting. The amount of ceramide and sphingomyelin was expressed as a percentage of the total lipid tritium in the sample.

Statistical Analysis

Data were analyzed by one- and two-way analysis of variance (ANOVA), and specific hypotheses were tested by the F statistic using pooled variances. Time and dose effects were tested by first-order polynomial contrasts. All statistical tests were two-sided. Statistical procedures were done using Systat, version 10 (SPSS, Chicago, IL). Data shown in the figures are means with 95% confidence intervals. The majority of experiments were done in triplicate, but some ds-siRNA experiments were done in duplicate only; data for these are presented as means with ranges.

Results

Effect of Inhibitors of Sphingomyelinase and Ceramide Synthase on Fenretinide-Induced ROS Generation and Apoptosis

Fumonisin B_1, an inhibitor of ceramide synthase *(31)*, reduces differentiation of SH-SY5Y cells *(32)* and inhibits apoptosis of other neuronal cells *(33)*. To assess whether ceramide synthase mediates fenretinide-induced ROS generation and apoptosis in neuroblastoma cells, SH-SY5Y and HTLA230 cells were incubated with fumonisin B_1 for 1 hour before they were incubated with fenretinide. In SH-SY5Y cells, 20 μ*M* fumonisin B_1 did not block fenretinide-induced ROS generation (Fig. 2, A) or apoptosis (Fig. 2, B). By contrast, fumonisin B_1 increased ROS and apoptosis in control cells (ANOVA, ROS, $F_{3,8} = 171.7$, $P<.001$; fumonisin B_1 versus control, $F_{1,8} = 10.1$, $P = .013$; apoptosis, $F_{5,12} = 118.1$, $P<.001$; fumonisin B_1 versus control, $F_{1,12} = 10.6$, $P = .007$). Fumonisin B_1 also increased ROS in combination with fenretinide ($F_{1,8} = 16.6$, $P<.05$) but had no effect on apoptosis in combination with fenretinide, regardless of fenretinide concentration ($F_{1,8} \leq 3.05$, $P>.1$). Similar results were obtained with the HTLA230 cells (data not shown).

We next tested the effects of other inhibitors of ceramide metabolism on fenretinide-induced ROS generation and apoptosis. Desipramine, an inhibitor of acidic and neutral sphingomyelinases *(16)*, effectively blocked fenretinide-induced ROS (Fig. 2, C; ANOVA, $F_{3,8} = 126.4$, $P<.001$; effect of desipramine on fenretinide response, $F_{1,8} = 225.5$, $P<.001$) and fenretinide-induced apoptosis (Fig. 2, D; fenretinide versus control, $F_{3,8} = 51.3$, $P<.001$; effect of desipramine on fenretinide response, $F_{1,8} = 101.5$, $P<.001$).

A study of hippocampal neurons has suggested that ceramide generated by neutral sphingomyelinase may be important for neuronal apoptosis *(34)*. To distinguish between neutral and acidic sphingomyelinase as mediators of fenretinide-induced apoptosis, SH-SY5Y cells were incubated with a neutral sphingomyelinase spirepoxide inhibitor for 1 hour before they were incubated with fenretinide. Treatment with the neutral sphingomyelinase spirepoxide inhibitor, unlike treatment with desipramine, did not block fenretinide-induced ROS (Fig. 2, E;

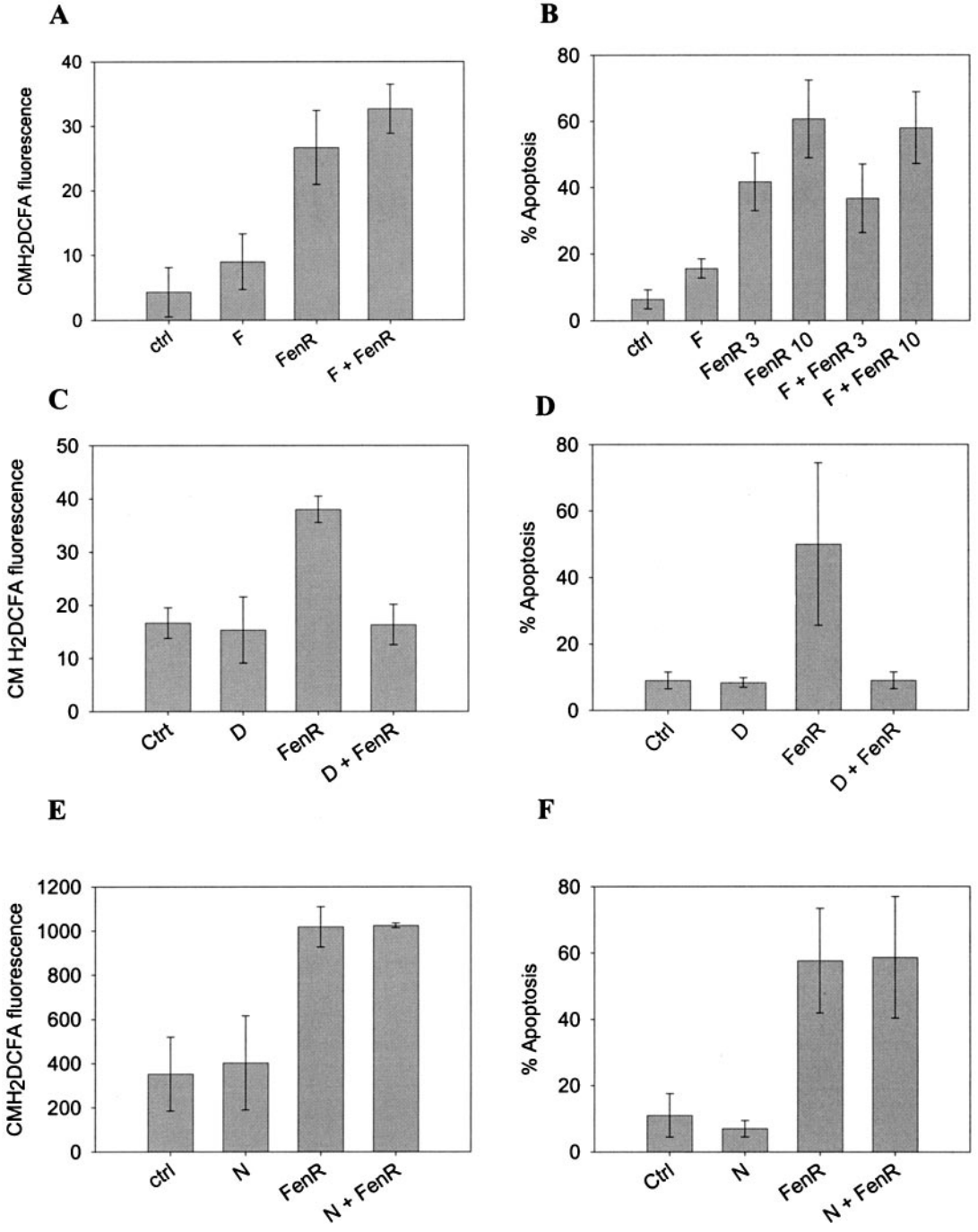

Fig. 2. Effect of fumonisin B_1, desipramine, and neutral sphingomyelinase spiroepoxide inhibitor on fenretinide-induced reactive oxygen species (ROS) generation and apoptosis in neuroblastoma cells. SH-SY5Y cells were treated with various inhibitors or control diluents for 1 hour and were then treated with fenretinide for 24 hours. ROS and apoptosis were measured by flow cytometry after 6 hours and 24 hours of treatment, respectively, as described *(10,11)*. Fenretinide-induced (FenR) ROS (**A**, **C**, **E**; ordinate CMH_2DCFA fluorescence) or apoptosis (**B**, **D**, **F**; ordinate % Apoptosis) of SH-SY5Y cells in the presence or absence of 20 μ*M* fumonisin B_1 ("F"; **A** and **B**), 5 μ*M* desipramine ("D"; **C** and **D**), or 1 μ*M* neutral sphingomyelinase spiroepoxide inhibitor ("N"; **E** and **F**). Fumonisin B_1 was added in ethanol, and desipramine or neutral sphingomyelinase spiroepoxide inhibitor was added in dimethyl sulfoxide. Fenretinide was added in ethanol with an equal volume of ethanol added to control cells. Fenretinide at 5 μ*M* was used in **A**, **C**, **D**, **E**, and **F.** For experiments to measure apoptosis in the presence or absence of fumonisin B_1 (**B**), fenretinide was added to final concentrations of either 3 μ*M* (FenR 3) or 10 μ*M* (FenR 10). For ROS measurements, data are presented as raw data in arbitrary units; the ordinate scale varies in magnitude according to amplifier settings for different sessions on the flow cytometer. Each bar in **A**–**F** is the mean with 95% confidence intervals for three replicates from a single experiment.

ANOVA, $F_{3,8} = 125.2$, $P<.001$; effect of neutral sphingomyelinase spirepoxide inhibitor on fenretinide-induced ROS, $F_{1,8} = 0.02$, $P>.8$) or fenretinide-induced apoptosis (Fig. 2, F; ANOVA, $F_{3,8} = 94.5$, $P<.001$; effect of neutral sphingomyelinase spirepoxide inhibitor on fenretinide-induced apoptosis, $F_{1,8} = 0.06$, $P>.8$) of SH-SY5Y cells. Thus acidic sphingomyelinase, but not neutral sphingomyelinase, is important in fenretinide-induced apoptosis of SH-SY5Y cells.

Acidic Sphingomyelinase Activity in Relation to Fenretinide-Induced Ceramide, Apoptosis, and ROS

To investigate further the role of acidic sphingomyelinase in fenretinide-induced apoptosis, RNA interference was used to reduce the expression of acidic sphingomyelinase. Compared with activity in untransfected SH-SY5Y cells or SH-SY5Y cells transfected with a control ds-siRNA, acidic sphingomyelinase activity was reduced by at least 50% in cells transfected with the acidic sphingomyelinase ds-siRNA (target sequence 18; Table 1 and Fig. 3, A). Western blotting of protein extracts from these cells confirmed a reduction in acidic sphingomyelinase protein in both control and fenretinide-treated SH-SY5Y cells transfected with the acidic sphingomyelinase ds-siRNA (Fig. 3, B). The western blot also revealed that acidic sphingomyelinase protein levels increased in response to treatment with 5 μ*M* fenretinide for 24 hours in control cells and cells transfected with the control ds-siRNA (Fig. 3, B). Thus, the western blot data (Fig. 3, B) and the slight increase in acidic sphingomyelinase activity in response to a 4-hour treatment with 5 μ*M*

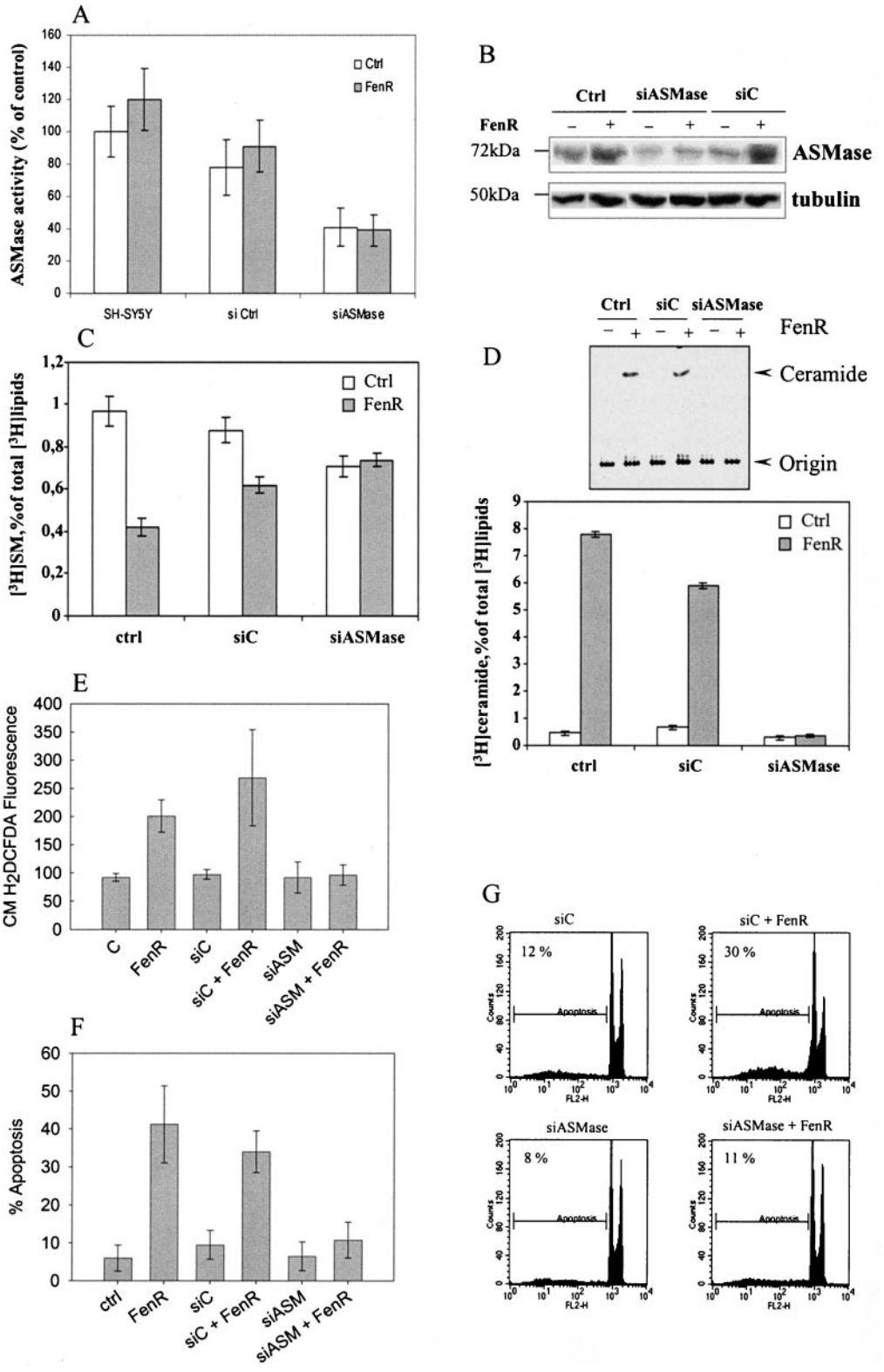

Fig. 3. Effect of inhibiting acidic sphingomyelinase activity by RNA interference in SH-SY5Y neuroblastoma cells. **A**) Acidic sphingomyelinase activity (expressed as a percentage of the activity of control untreated and untransfected cells) in SH-SY5Y cells treated with 5 μ*M* fenretinide (FenR) or the ethanol diluent (Ctrl) for 4 hours, and in SH-SY5Y cells transfected with either a double-stranded small interfering RNA (ds-siRNA) for acidic sphingomyelinase (siASMase) or a control ds-siRNA (siC) and treated with 5 μ*M* fenretinide or its diluent (ethanol) for 4 hours. Each bar is the mean and range of duplicate samples from a single experiment. **B**) Western blot analysis of whole-cell lysates for SH-SY5Y cells (Ctrl) treated with 5 μ*M* fenretinide (FenR, +) or ethanol (–) for 24 hours, and for SH-SY5Y cells transfected with ds-siRNA for ASMase (siASMase) or control ds-siRNA sequence (siC) and treated with 5 μ*M* fenretinide (FenR, +) or ethanol (–) for 24 hours. Immunoblots were probed sequentially for ASMase and β-tubulin. Sphingomyelin levels (**C**) expressed as a percentage of total [^{3}H]-labeled lipids, and ceramide (**D**) shown as bands separated by thin-layer chromatography (**upper panel**) and as a percentage of total [^{3}H]-labeled lipids (**lower panel**), in SH-SY5Y cells treated with 5 μ*M* fenretinide (FenR) or ethanol for 18 hours (Ctrl), and in SH-SY5Y cells transfected with ds-siRNA for ASMase (siASMase) or control ds-siRNA sequence (siC) and treated with 5 μ*M* fenretinide (FenR) or ethanol for 18 hours; each bar is the mean ± range of duplicate samples. Reactive oxygen species (ROS; **E**) and apoptosis (**F**) were measured by flow cytometry, as described *(10,11)*. ROS induction (CMH_2DCFDA Fluorescence, ordinate) after 6 hours and apoptosis after 24 hours in SH-SY5Y cells treated with 5 μ*M* fenretinide (FenR) or ethanol ("C"), and in SH-SY5Y cells transfected with ds-siRNA for ASMase (siASM) or control ds-siRNA sequence (siC) and treated with 5 μ*M* fenretinide (FenR) or ethanol. Each bar is mean (± 95% confidence intervals) of triplicate samples in (**E**) and of quadruplicate samples in (**F**). **G**) Representative flow cytometry profiles of SH-SY5Y cells transfected with a control ds-siRNA (siC) or ds-siRNA for ASMase (siASMase) and treated with 5 μ*M* fenretinide (FenR) or ethanol for 24 hours. The inset percentages show the percentage of apoptotic cells.

fenretinide (Fig. 3, A) suggest that fenretinide increased acidic sphingomyelinase levels in SH-SY5Y cells and that the acidic sphingomyelinase ds-siRNA effectively reduced the expression of both constitutive and fenretinide-induced acidic sphingomyelinase.

We then asked whether increased activity and expression of acidic sphingomyelinase is important in fenretinide-induced apoptosis of SH-SY5Y cells by measuring sphingomyelin levels and cellular ceramide levels after fenretinide treatment. We reasoned that, if acidic sphingomyelinase was important, then sphingomyelin levels would decrease and ceramide levels would increase. Indeed, sphingomyelin levels, expressed as a percentage of total [^{3}H]-labeled lipids, decreased in SH-SY5Y cells after treatment with fenretinide (Fig. 3, C), and this decrease was blocked in cells transfected with acidic sphingomyelinase ds-siRNA (Fig. 3, C). Conversely, ceramide levels increased in

SH-SY5Y cells after treatment with fenretinide (Fig. 3, D), and this increase was blocked in cells transfected with acidic sphingomyelinase ds-siRNA but not with the control ds-siRNA (Fig. 3, D). Fenretinide-induced apoptosis and ROS were inhibited in SH-SY5Y cells transfected with the acidic sphingomyelinase ds-siRNA but not in cells transfected with the control ds-siRNA (Fig. 3, E–G). ROS levels were higher in cells transfected with the control ds-siRNA and treated with fenretinide than in control cells treated with fenretinide alone (ANOVA, $F_{5,12} = 68.3$, $P<.001$; fenretinide versus fenretinide plus control ds-siRNA, $F_{1,12} = 27.5$, $P<.001$). By contrast, ROS levels were similar among control cells, cells transfected with acidic sphingomyelinase ds-siRNA, and cells transfected with acidic sphingomyelinase ds-siRNA and treated with fenretinide, suggesting that the acidic sphingomyelinase ds-siRNA completely blocked fenretinide-induced ROS (fenretinide versus fenretinide plus acidic sphingomyelinase-specific ds-siRNA, $F_{1,12} = 65.2$, $P<.001$).

Levels of fenretinide-induced apoptosis in cells transfected with the control ds-siRNA did not differ from levels in fenretinide-treated control cells (ANOVA, $F_{5,18} = 39.0$, $P<.001$; fenretinide versus fenretinide with control ds-siRNA, $F_{1,18} = 1.7$, $P = .215$). However, levels of fenretinide-induced apoptosis in cells transfected with acidic sphingomyelinase ds-siRNA were similar to levels in untreated (i.e., no fenretinide) control cells ($F_{1,18} = 49.5$, $P<.001$).

Glucosylceramide Synthase Activity and Gangliosides GD3 and GD2 After Fenretinide Treatment

Sphingomyelinase-generated ceramide is a substrate for glucosylceramide synthase, the activity of which results in the formation of glycosphingolipids and gangliosides, including the disialogangliosides GD3 and GD2. To test whether GD3 and GD2 may be downstream effectors of fenretinide-induced apoptosis, we assessed whether glucosylceramide synthase activity changed over time in response to fenretinide treatment and measured the effects of a glucosylceramide synthase inhibitor, PDMP, on fenretinide-induced apoptosis. Glucosylceramide synthase activity increased in a time-dependent manner during the first 6 hours after the addition of fenretinide (ANOVA, $F_{3,8} = 126.7$, $P<.001$; effect of time: first-order polynomial contrast, $F_{1,8} = 342.1$, $P<.001$) (Fig. 4, A).

PDMP, a specific inhibitor of glucosylceramide synthase, at concentrations of 10, 20, or 30 μ*M* was added to SH-SY5Y cells 1 hour before treatment with fenretinide for 24 hours (two-way ANOVA: PDMP, fenretinide, and PDMP–fenretinide interaction, $F_{3,16} = 60.8$, $F_{1,16} = 260.7$, and $F_{3,16} = 72.4$, respectively, $P<.001$). Compared with SH-SY5Y cells that did not receive the inhibitor, fenretinide-induced apoptosis was reduced by approximately 5% in cells treated with the lowest PDMP concentration (10 μ*M*) ($F_{1,16} = 5.4$, $P = .033$). However, fenretinide-induced apoptosis was completely blocked in cells treated with 20 and 30 μ*M* PDMP (Fig. 4, B; $F_{1,16}>187.0$, $P<.001$).

Evidence from other studies *(21,35)* has suggested that the hydrolysis of sphingomyelin via sphingomyelinase increases levels of GD3 and that GD3 is a critical signaling intermediate in the apoptosis of lymphoid and neuronal cells. Therefore, it is possible that GD3 may increase in SH-SY5Y neuroblastoma cells as a result of a fenretinide-induced increase in glucosylceramide synthase activity, and that this GD3 rise is responsible

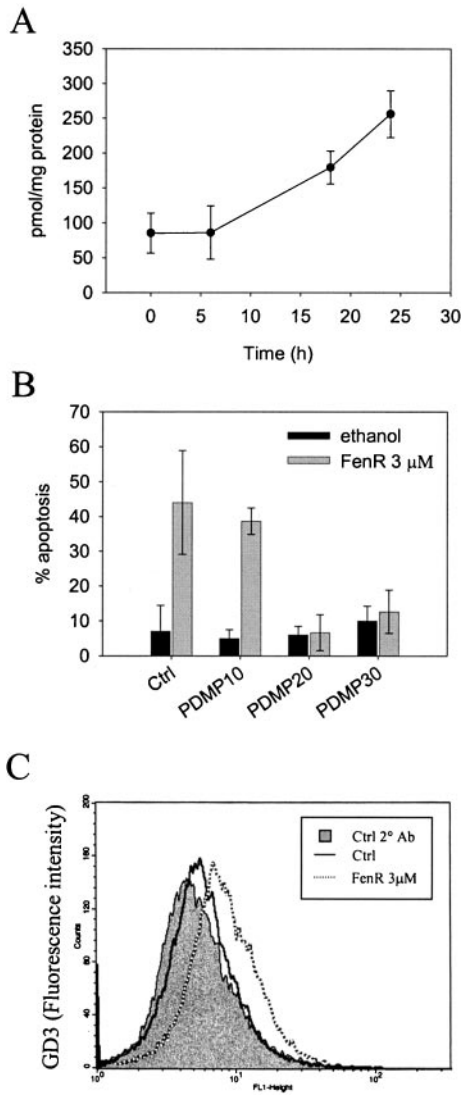

Fig. 4. Fenretinide-induced glucosylceramide synthase activity and ganglioside GD3 accumulation. **A**) Time course of glucosylceramide synthase activity (picomole of glucosylceramide–NBD per milligram of protein, ordinate) in SH-SY5Y neuroblastoma cells treated with 5 μ*M* fenretinide. Each point is the mean of triplicate samples with 95% confidence intervals. **B**) Percentage of apoptosis (ordinate) of SH-SY5Y cells treated with 3 μ*M* fenretinide or its diluent (ethanol) in the presence or absence of the glucosylceramide synthase inhibitor 1-phenyl-2-decanoylamino-3-morpholino-1-propanol (PDMP). PDMP was added in dimethyl sulfoxide to concentrations of 10 μ*M*, 20 μ*M*, or 30 μ*M*, with an equal volume of dimethyl sulfoxide used to treat control cells, 1 hour before treatment with 3 μ*M* fenretinide or ethanol. Each bar is the mean of triplicate samples with 95% confidence intervals. **C**) Representative flow cytometry immunofluorescence profiles for expression of the ganglioside GD3 in control SH-SY5Y cells (**solid black line**) and in SH-SY5Y cells treated for 24 hour with 3 μ*M* fenretinide (FenR; **dotted line**). As a control for nonspecific immunofluorescence, cells were stained with the secondary antibody alone (**shaded profile**).

for subsequent events leading to apoptosis. To test this possibility, we used immunofluorescence flow cytometry to measure levels of GD3 in SH-SY5Y cells after treatment with fenretinide. As shown in Fig. 4, C, we found that GD3 levels increased twofold in response to fenretinide treatment ($F_{1,11} = 12.6$, $P = .005$). GD3 is the first member of the b-series gangliosides and generates GD2 via the addition of *N*-acetylgalactosamine *(36)*. Therefore, immunofluorescence flow cytometry with an anti-

GD2 antibody was used to determine whether GD2 also increases in response to fenretinide. Compared with GD2 levels in untreated SH-SY5Y cells, levels of GD2 in SH-SY5Y cells increased 2.5-fold in response to fenretinide under the same conditions used for the GD3 experiments (Fig. 5).

Effect of Blocking the Induction of GD3 on Fenretinide-Induced ROS and Apoptosis

GD3 is generated from the monosialoganglioside GM3 by the enzyme α-*N*-acetylneuraminate α-2,8-sialyltransferase (GD3 synthase). To determine whether this enzyme is necessary for fenretinide-induced apoptosis, ds-siRNAs were designed to reduce the expression of GD3 synthase in SH-SY5Y cells. All three ds-siRNAs, targeting different sequences of GD3 synthase mRNA (Table 1), were effective in blocking fenretinide-induced apoptosis after transfection into SH-SY5Y cells (Fig. 6, A). One of these (ds-siRNA43) was used for further experiments. The fenretinide-induced increase in cellular GD3 levels was effectively blocked in cells transfected with ds-siRNA43 (ANOVA, $F_{5,11} = 43.4$, $P<.001$; GD3 synthase siRNA and fenretinide treatment versus control SH-SY5Y cells and fenretinide, $F_{1,11} = 70.0$, $P<.001$; Fig. 6, B and C). This result is indirect evidence that the ds-siRNA43 probe was effective in reducing GD3 synthase activity. Compared with untransfected cells treated with fenretinide, cells transfected with the control ds-siRNA had increased GD3 levels in response to fenretinide ($F_{1,11} = 14.9$, $P = .003$). Levels of fenretinide-induced apoptosis in cells transfected with the GD3 synthase ds-siRNA43 were reduced to the levels seen in untreated control cells (Fig. 6, D and F; ANOVA, $F_{5,12} = 33.2$, $P<.001$; effect of control ds-siRNA on fenretinide-induced apoptosis, $F_{1,12} = 3.1$, $P>.1$; effect of GD3 synthase-specific ds-siRNA on fenretinide-induced apoptosis, $F_{1,12} = 86.9$, $P<.001$). Furthermore, the fenretinide-dependent increase in ROS was blocked in cells transfected with ds-siRNA43 but not in cells transfected with control ds-siRNA (Fig. 6, E; ANOVA, $F_{5,12} = 267.3$, $P<.001$; fenretinide versus fenretinide plus control ds-siRNA, $F_{1,12} = 0.3$, $P>.5$; fenretinide versus fenretinide plus GD3 synthase-specific ds-siRNA, $F_{1,12} = 388.8$, $P<.001$). These data suggest that GD3 synthase mediates fenretinide-induced apoptosis and ROS generation via the production of increased levels of GD3.

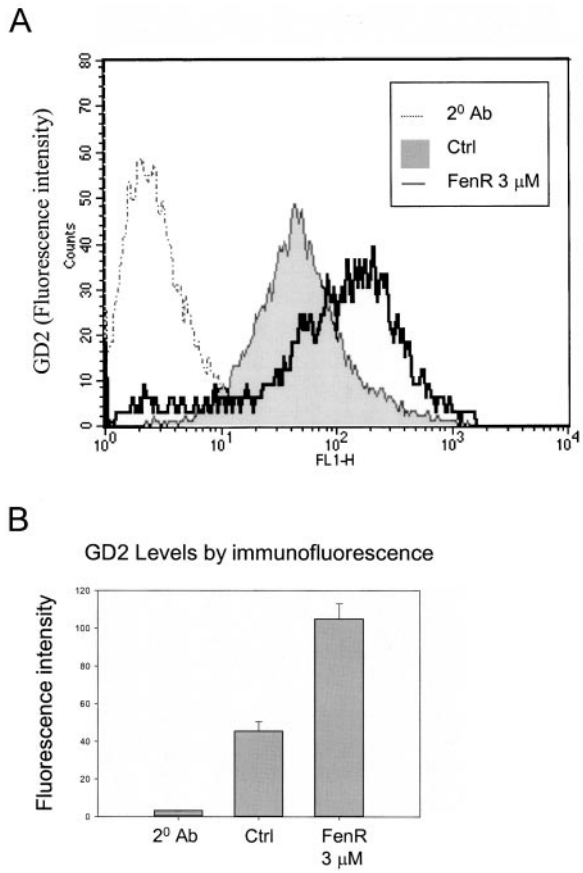

Fig. 5. Expression of the ganglioside GD2 in SH-SY5Y neuroblastoma cells. **A**) Flow cytometry immunofluorescence profiles for expression of GD2 in control SH-SY5Y cells (**shaded profile**) and in SH-SY5Y cells treated for 24 hours with 3 μ*M* fenretinide (FenR; **solid line**). As a control for nonspecific immunofluorescence, cells were stained with the secondary antibody alone (**dotted line**). **B**) GD2 levels were measured and quantified by fluorescein isothiocyanate–fluorescence intensity (ordinate) from flow cytometry of SH-SY5Y cells stained with an anti-GD2 antibody after treatment with 3 μ*M* fenretinide for 24 hours (FenR) or its diluent (ethanol; Ctrl). Results from samples stained with the secondary antibody alone (2^0 Ab) are also shown. Each bar is the mean with upper bound of range of duplicate samples.

Apoptosis of SH-SY5Y Cells in Response to Exogenous Gangliosides

The addition of exogenous GD3 at concentrations up to 10 μ*M* to cultures of smooth muscle cells stimulates ROS and apoptosis *(37)*. Neuroblastoma cells have high levels of endogenous GD2 *(38)*. We added exogenous GD3 or GD2 (at concentrations of 1, 5, and 10 μ*M*) to SH-SY5Y cultures to determine whether these gangliosides would mimic the effects of fenretinide with respect to the induction of ROS and apoptosis. Apoptosis increased dose-dependently after treatment with GD3 (two-way ANOVA, control and GD3 treatments, effects of time and treatment, $F_{1,16} = 26.5$, $P<.001$ and $F_{3,16} = 261.1$, $P<.001$, respectively; first-order polynomial contrast on GD3 dose, $F_{1,16} = 763.1$, $P<.001$), with 10 μ*M* GD3 inducing 40% apoptosis and 5 μ*M* fenretinide inducing 55% apoptosis at 24 hours (Fig. 7, A). Similar results were obtained with GD3-induced ROS (first-order polynomial contrast, effect of GD3 dose, $F_{1,16} = 136.4$, $P<.001$; Fig. 7, B).

We showed previously that 12-lipoxygenase activity is increased and necessary for fenretinide-induced apoptosis in SH-SY5Y cells *(11)*, and it has been reported that GD3 can increase 12-lipoxygenase activity in human lymphocytes *(39)*. Therefore, if GD3 is an intermediate on the biochemical pathway leading to ROS generation and apoptosis after fenretinide treatment, we would expect these effects of GD3 to be blocked by lipoxygenase inhibitors. As shown in Fig. 7, C and D, apoptosis and ROS levels were similar in SH-SY5Y cells cultured with the specific 12-lipoxygenase inhibitor baicalein (1 μ*M*) and in untreated control cells. However, both fenretinide-induced and GD3-induced apoptosis (measured after 24 hours) and fenretinide-induced and GD3-induced ROS generation (measured after 6 hours) were blocked in SH-SY5Y cells cultured with baicalein (1 μ*M*) added 2 hours before the addition of fenretinide (5 μ*M*) or exogenous GD3 (5 μ*M*) (ANOVA, $F_{5,12} = 73.3$ and $F_{5,12} = 812.3$ for apoptosis and ROS, respectively, $P<.001$ for both; effects of GD3 versus GD3 plus baicalein, $F_{1,12}>105.0$ for apoptosis and ROS, $P<.001$ for both).

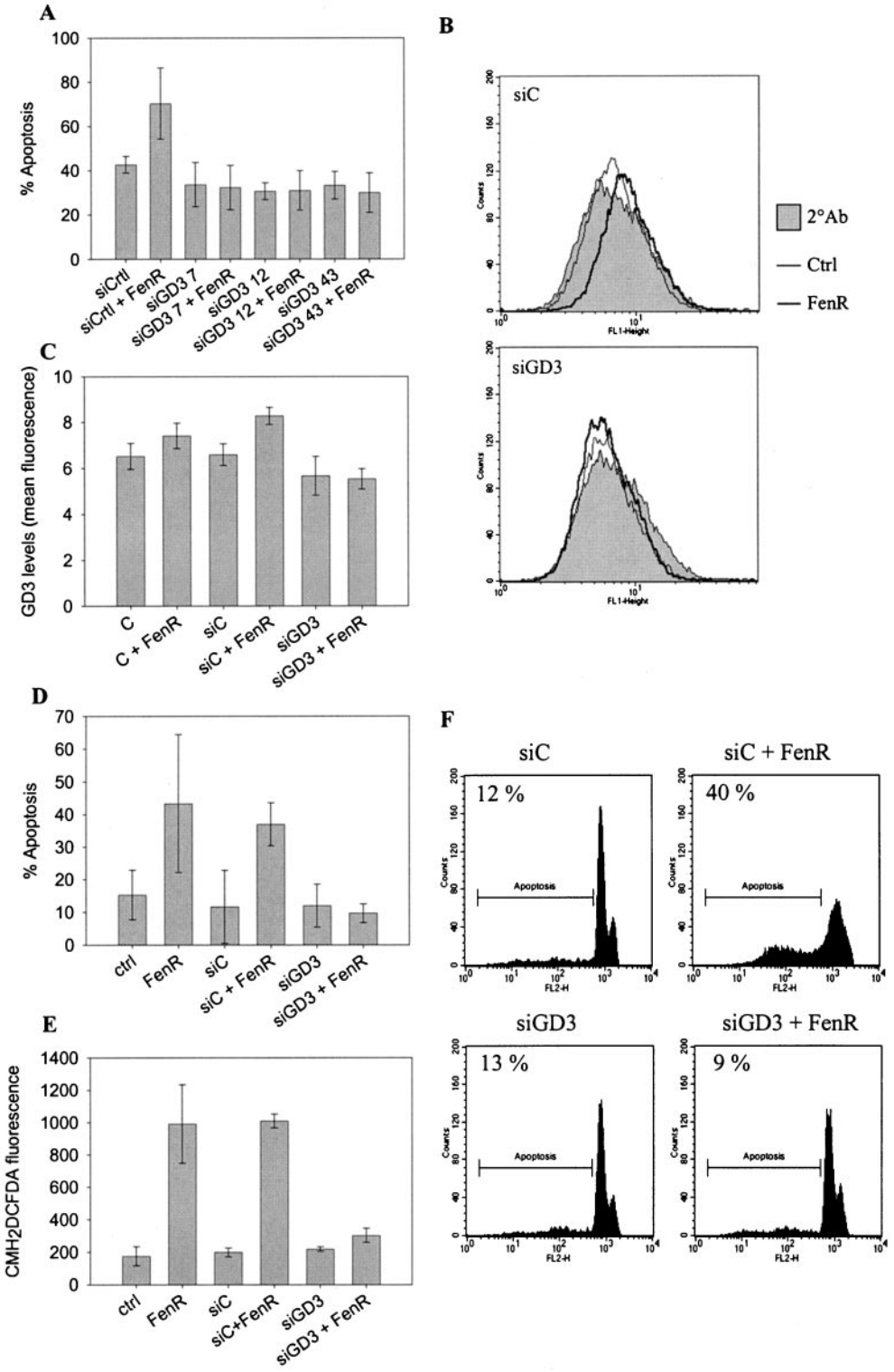

Fig. 6. Effect of RNA interference for GD3 synthase. **A**) Apoptosis, measured by flow cytometry *(10,11)*, of SH-SY5Y cells transfected with a control double-stranded small interfering RNA (ds-siRNA, siC) or three different ds-siRNAs for GD3 synthase (numbered 7, 12, or 43), and treated with 5 μ*M* fenretinide or its diluent (ethanol) for 24 hours. Each bar is the mean of triplicate samples with 95% confidence intervals. **B**) Flow cytometry immunofluorescence profiles for the expression of the ganglioside GD3 in SH-SY5Y cells transfected with control ds-siRNA (siC) or with the GD3 synthase ds-siRNA43 and subsequently treated for 24 hours with 5 μ*M* fenretinide (FenR; **solid thick line**) or ethanol (Ctrl; **solid thin line**). As a control for nonspecific immunofluorescence, cells were stained with the secondary antibody alone (**shaded profile**). GD3 levels (**C**), apoptosis (**D**), and reactive oxygen species (ROS; **E**) were measured by flow cytometry in SH-SY5Y cells after treatment with 5 μ*M* fenretinide (FenR) for 24 hours or ethanol (ctrl), and in cells transfected with ds-siRNA43 for GD3 synthase (siGD3) or control ds-siRNA (siC) and treated with 5 μ*M* fenretinide or ethanol for 24 hours. ROS was measured after 6 hours. Each bar is mean of triplicate samples with 95% confidence intervals, with the exception of the untransfected vehicle control cells, which were in run in duplicate. **C**) Ordinate = fluorescence (arbitrary units). **D**) Ordinate = percent apoptosis. **E**) Ordinate = fluorescence (arbitrary units). **F**) Flow cytometry profiles showing the percent of apoptotic cells (inset number) among SH-SY5Y cells transfected with ds-siRNA43 for GD3 synthase (siGD3) or control ds-siRNA (siC) and treated with 5 μ*M* fenretinide (FenR) or ethanol for 24 hours. Representative profiles are shown.

In contrast to the effects of GD3, GD2 did not induce apoptosis of SH-SY5Y cells; indeed, there was an overall reduction in the percentage of apoptosis with increased time of treatment (Fig. 7, E; two-way ANOVA on GD2 and control treatments: effect of time, $F_{1,24} = 31.3$, $P<.001$; effect of GD2, $F_{5,24} = 1.4$, $P>0.2$; no time–GD2 interaction, $F_{5,24} = 0.5$, $P>.7$). Baicalein had no effect on apoptosis in cells treated with GD2 (Fig. 7, E). These results suggest that the apoptotic effects of GD3 were not a result of subsequent metabolism to GD2.

Discussion

The results of this study suggest that gangliosides derived from ceramide metabolism are essential signaling intermediates in fenretinide-induced apoptosis of SH-SY5Y cells, leading to the induction of ROS via 12-lipoxygenase. The effects of sphingomyelinase inhibitors indicate that acidic sphingomyelinase activity is required for apoptosis in SH-SY5Y and HTLA230 neuroblastoma cells in response to fenretinide, and this finding

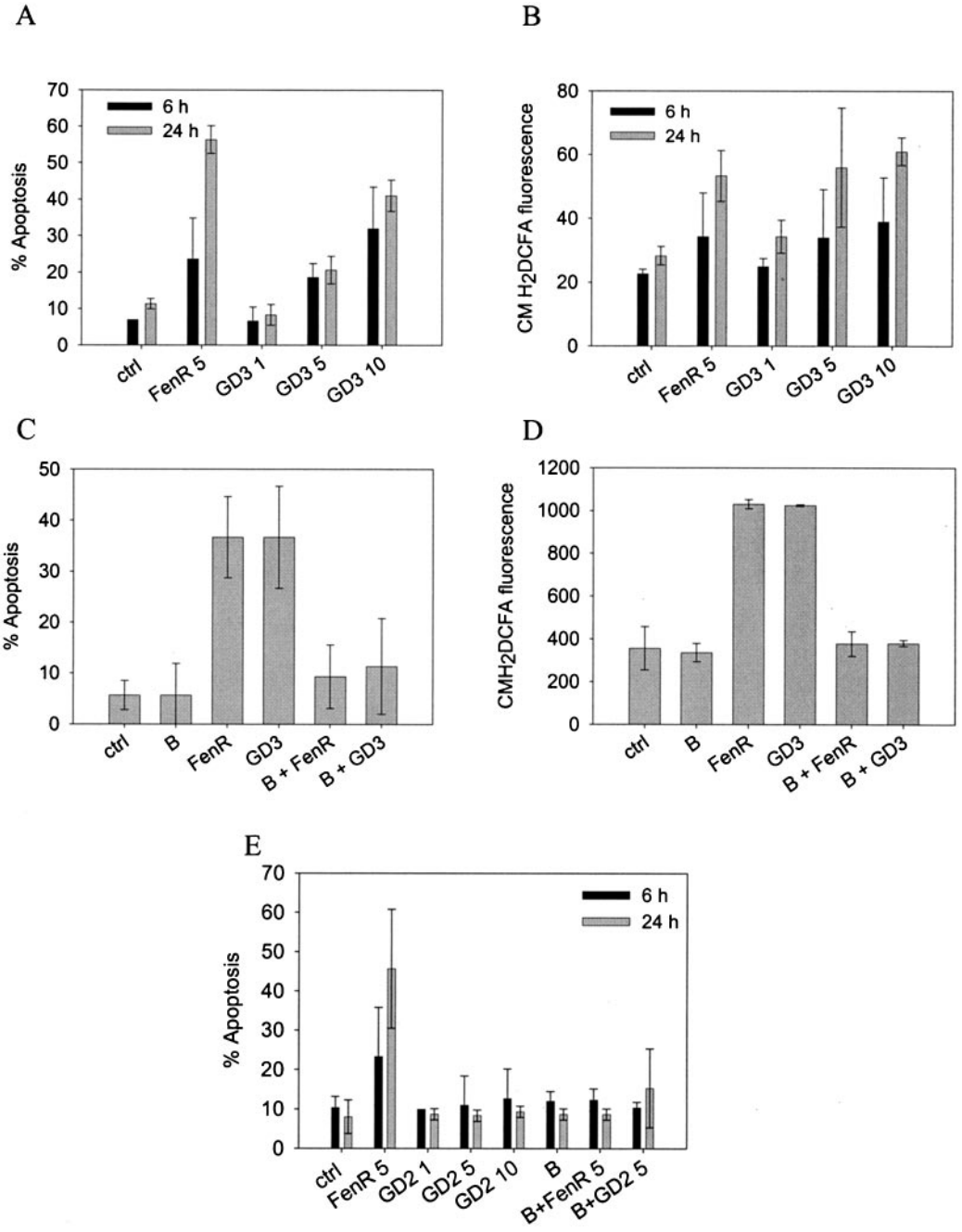

Fig. 7. Reactive oxygen species (ROS) and apoptosis in SH-SY5Y cells treated with exogenously provided gangliosides GD3 and GD2. ROS and apoptosis were measured by flow cytometry. **A**) Induction of apoptosis of SH-SY5Y cells after treatment with 5 μ*M* fenretinide (FenR 5 μ*M*) or 1 μ*M* (GD3 1μ*M*), 5 μ*M* (GD3 5 μ*M*), or 10 μ*M* (GD3 10 μ*M*) exogenous GD3 (GD3) or the diluent (ethanol; Ctrl) for 6 or 24 hours. **B**) Induction of ROS in SH-SY5Y cells after treatment with 5 μ*M* fenretinide or 1, 5, or 10 μ*M* exogenous GD3 (abscissa labels as in A) for 2 or 6 hours. **C**) Induction of apoptosis of SH-SY5Y cells after treatment with 1 μ*M* baicalein ("B") or its diluent (ethanol; ctrl) for 2 hours followed by treatment with 5 μ*M* fenretinide, 5 μ*M* GD3, or ethanol for 24 hours. **D**) Induction of ROS in SH-SY5Y cells after sequential treatment with 1 μ*M* baicalein ("B") or ethanol for 2 hours and 5 μ*M* fenretinide, 5 μ*M* GD3, or ethanol for 6 hours. **E**) Induction of apoptosis in SH-SY5Y cells after treatment for 6 or 24 hours with 5 μ*M* fenretinide (FenR) or with 1 μ*M* (GD2 1 μ*M*), 5 μ*M* (GD2 5 μ*M*), or 10 μ*M* (GD2 10 μ*M*) exogenously provided GD2 or with ethanol (ctrl). In addition, some cells were sequentially treated with 1 μ*M* baicalein ("B") for 2 hours and 5 μ*M* fenretinide (FenR 5 μ*M*) or 5 μ*M* GD2 (GD2 5 μ*M*) for 4 or 22 hours. In each panel, each bar represents the mean of triplicate samples with 95% confidence intervals.

was confirmed by using ds-siRNA probes to knock down acidic sphingomyelinase activity. These data confirm results for other cell lines that ceramide increases *(5,40)* during fenretinide-induced apoptosis and suggest that, in SH-SY5Y and HTLA230 neuroblastoma cells, ceramide is derived from sphingomyelin via sphingomyelinase activity. The involvement of sphingomyelinases may explain the observation that fumonisin B_1, an inhibitor of ceramide synthase, was relatively ineffective at blocking fenretinide-induced apoptosis of CHLA-90 and SK-N-RA neuroblastoma cells *(14)* but is at odds with the finding that sphingomyelin levels increase in these neuroblastoma cells after fenretinide treatment *(14)*. Clearly, the results for SH-SY5Y and HTLA230 neuroblastoma cells differ from those of other studies indicating that fenretinide increases ceramide levels via the *de novo* synthesis pathway in which serine palmitoyltransferase and ceramide synthase are key elements. Because fenretinide has been used in other studies at concentrations that induce necrosis and apoptosis *(5)*, it is possible that both *de novo* synthesis and sphingomyelinase pathways are activated in response to fenretinide but that these relate to different cell death–signaling pathways.

The mechanism of either acidic sphingomyelinase or serine–palmitoyltransferase activation in response to fenretinide in any cell type is currently unknown. In addition to inducing oxidative stress, or ROS, fenretinide is an RARβ/γ agonist. We have argued that both ROS-dependent and RAR-dependent pathways are necessary for fenretinide-induced apoptosis of SH-SY5Y cells on the basis of evidence that RARβ/γ antagonists block fenretinide-induced apoptosis but do not block ROS induction *(10)*. In NB4 acute promyelocytic leukemia cells, retinoic acid induces acidic sphingomyelinase via retinoic acid response elements within the acidic sphingomyelinase promoter *(41)*. The

rate-limiting enzyme in the *de novo* synthesis pathway, serine–palmitoyltransferase, can also be activated, albeit at a post-translational level, by retinoic acid during neuronal differentiation *(33)*. Therefore, the induction of acidic sphingomyelinase by fenretinide in SH-SY5Y cells may be mediated by RARs. Alternatively, acidic sphingomyelinase activation could be dependent on Fas-associated protein with death domain and result from an increase in the rate of substrate hydrolysis, as in embryonic fibroblasts *(42)*.

Evidence suggests that ceramide can induce apoptosis in cells through different mechanisms, either directly as a lipid-signaling molecule interacting with enzyme systems that participate in apoptosis regulation or by further metabolism to other lipid mediators, such as gangliosides *(43)*. The data for SH-SY5Y cells imply that glucosylceramide synthase and GD3 synthase, key elements in the synthesis of gangliosides from ceramide, are essential steps in apoptosis and ROS generation in response to fenretinide. Glucosylceramide synthase activity showed a linear, time-dependent increase in response to fenretinide, and this activity may result from the transcriptional induction of glucosylceramide synthase, possibly mediated by nuclear factor-κB *(44)*, and/or by post-translational activation *(45,46)* in response to increasing ceramide levels. In CHP-100 neuroepithelioma cells, blocking glucosylceramide synthase expression with an antisense construct decreases sensitivity to fenretinide-induced apoptosis *(29)*. This supports the role of glucosylceramide synthase in mediating fenretinide-induced apoptosis of SH-SY5Y cells and suggests that this ceramide signaling pathway also mediates fenretinide-induced cell death in other cell types. By contrast, the overexpression of glucosylceramide synthase has been associated with resistance to chemotherapeutic drugs in neuroblastoma and other tumors *(47,48)*. Although inhibitors of glucosylceramide synthase reportedly act synergistically with fenretinide in CHLA-90 neuroblastoma cells *(14)*, such chemosensitizing effects may be independent of the activity of these compounds as glucosylceramide synthase inhibitors *(47)*. Nevertheless, the complexity of these lipid signaling pathways is highlighted by the fact that inhibition of glucosylceramide synthase can increase apoptosis in CHP-100 cells but that blocking this enzyme with an antisense construct does not affect the response to p53-dependent apoptotic drugs *(49)*. Clearly, altering the metabolic flux of sphingolipid metabolism can induce apoptosis by a variety of mechanisms, including ceramide accumulation, perhaps leading to necrosis *(14)* or ganglioside synthesis.

Glucosylceramide is metabolized via galactosyl transferase to lactosylceramide, and the subsequent activity of different sialyltransferases generates the first intermediates of the a-, b- and c-series gangliosides (Fig. 1) *(36)*. The abrogation of fenretinide-induced apoptosis and ROS generation by knockdown of GD3 synthase suggests that the b- and c-series gangliosides are signaling intermediates of ceramide metabolism. Although the ganglioside GT3, the first member of the c-series gangliosides, has growth-regulatory properties, it may be synthesized within a different compartment of the Golgi than GD3, giving greater weight to the idea that GD3, or a subsequent member of the b-series gangliosides, such as GD2, is the primary messenger. However, although GD2 levels were also increased by fenretinide, this b-series ganglioside did not induce apoptosis. Therefore, GD3 is probably the main ganglioside of the apoptotic signaling pathway induced by fenretinide. Although the effects of exogenous GD3 may be different from those of GD3 generated by intracellular metabolism *(37)*, two recent studies illustrate the importance of GD3 in apoptotic signaling. Bhunia et al. *(37)* demonstrated that the induction of high levels of GD3 induced ROS and triggered signaling events leading to apoptosis, and Copani et al. *(35)* suggested that GD3 contributes to the apoptosis of neuronal cells.

Substantial evidence indicates that GD3 can interact directly with mitochondria, stimulating apoptosis as a result of opening the mitochondrial permeability transition pore *(36)*. However, in SH-SY5Y neuroblastoma cells, fenretinide-dependent apoptosis is not mediated by the opening of the mitochondrial permeability transition pore, at least in the early stages of apoptosis *(10)*. Because the effects of exogenous GD3 on ROS generation and apoptosis were, as with fenretinide *(11)*, inhibited by the 12-lipoxygenase inhibitor baicalein, GD3 may be a signaling intermediate upstream of lipoxygenase activation. Although a direct link between gangliosides and lipoxygenase activation has not, to our knowledge, been established, GD3 can modulate 12-lipoxygenase activity in human peripheral blood lymphocytes *(39)*. Clearly, the relationships between gangliosides, lipoxygenase activity, and apoptotic control pathways deserve further investigation.

In summary, our results suggest that acidic sphingomyelinase mediates fenretinide-induced apoptosis in neuroblastoma cells and that the induction of the ganglioside GD3, resulting from glucosylceramide synthase and GD3 synthase activities, may link increased ceramide levels with 12-lipoxygenase activation and subsequent apoptosis. These data raise new questions about the role of gangliosides in fenretinide-induced apoptosis and in regulating lipoxygenase activity, and they identify new targets for the development of drugs to improve current therapy for neuroblastoma. Furthermore, the observation that GD2 levels increase in response to fenretinide suggests that the response of neuroblastoma to therapy with anti-GD2 antibodies might be increased by co-treatment with fenretinide.

REFERENCES

(1) Brodeur G. Neuroblastoma: biological insights into a clinical enigma. Nat Rev Cancer 2003;3:203–16.

(2) Matthay KK, Villablanca JG, Seeger RC, Stram DO, Harris RE, Ramsay NK, et al. Treatment of high risk neuroblastoma with intensive chemotherapy, radiotherapy, autologous bone marrow transplantation, and 13-cis retinoic acid. N Engl J Med 1999;341:1165–73.

(3) Lasorella A, Iavarone A, Israel MA. Differentiation of neuroblastoma enhances Bcl-2 expression and induces alterations of apoptosis and drug resistance. Cancer Res 1995;55:4711–6.

(4) Meister B, Fink FM, Hittmair A, Marth C, Widschwendter M. Antiproliferative activity and apoptosis induced by retinoic acid receptor-gamma selectively binding retinoids in neuroblastoma. Anticancer Res 1998;18:1777–86.

(5) Maurer BJ, Metelitsa LS, Seeger RC, Cabot MC, Reynolds CP. Increase of ceramide and induction of mixed apoptosis/necrosis by N-(4-hydroxyphenyl)-retinamide in neuroblastoma cell lines. J Natl Cancer Inst 1999;91:1138–46.

(6) Lovat PE, Ranalli M, Bernassola F, Tilby MJ, Malcolm AJ, Pearson AD, et al. Synergistic induction of apoptosis of neuroblastoma by fenretinide or CD437 in combination with chemotherapeutic drugs. Int J Cancer 2000;88:977–85.

(7) Lovat PE, Ranalli M, Bernassola F, Tilby M, Malcolm AJ, Pearson AD, et al. Distinct properties of fenretinide and CD437 lead to synergistic responses with chemotherapeutic reagents. Med Pediatr Oncol 2000;35:663–8.

(8) Sabichi AL, Modiano MR, Lee JJ, Peng YM, Xu MJ, Villar H, et al. Breast tissue accumulation of retinamides in a randomized short-term study of fenretinide. Clin Cancer Res 2003;9:2400–5.

(9) Garaventa A, Luksch R, Piccolo MS, Cavadini E, Montaldo PG, Pizzitola MR, et al. Phase I trial and pharmacokinetics of fenretinide in children with neuroblastoma. Clin Cancer Res 2003;9:2032–9.

(10) Lovat PE, Ranalli M, Annichiarrico-Petruzzelli M, Bernassola F, Piacentini M, Malcolm AJ, et al. Effector mechanisms of fenretinide-induced apoptosis in neuroblastoma. Exp Cell Res 2000;260:50–60.
(11) Lovat PE, Oliverio S, Ranalli M, Corrazzari M, Rodolfo C, Bernassola F, et al. GADD153 and 12-lipoxygenase mediate fenretinide-induced apoptosis of neuroblastoma. Cancer Res 2002;62:5158–67.
(12) Lovat PE, Ranalli M, Corazzari M, Raffaghello L, Pearson AD, Ponzoni M, et al. Mechanisms of free-radical induction in relation to fenretinide-induced apoptosis of neuroblastoma. J Cell Biochem 2003;89:698–708.
(13) Lovat PE, Oliverio S, Corazzari M, Rodolfo C, Ranalli M, Goranov B, et al. Bak: a downstream mediator of fenretinide-induced apoptosis of SH-SY5Y neuroblastoma cells. Cancer Res 2003;63:7310–3.
(14) Maurer BJ, Melton L, Billups C, Cabot MC, Reynolds CP. Synergistic cytotoxicity in solid tumor cell lines between N-(4-hydroxyphenyl) retinamide and modulators of ceramide metabolism. J Natl Cancer Inst 2000;92:1897–909.
(15) Wang H, Charles AG, Frankel AJ, Cabot MC. Increasing intracellular ceramide: an approach that enhances the cytotoxic response in prostate cancer cells. Urology 2003;61:1047–52.
(16) Erdreich-Epstein A, Tran LB, Bowman NN, Wang H, Cabot MC, Durden DL, et al. Ceramide signaling in fenretinide-induced endothelial cell apoptosis. J Biol Chem 2002;277:49531–7.
(17) Wang H, Maurer BJ, Reynolds CP, Cabot MC. N-(4-hydroxyphenyl) retinamide elevates ceramide in neuroblastoma cell lines by coordinate activation of serine palmitoyltransferase and ceramide synthase. Cancer Res 2001;61:5102–5.
(18) Hannun YA, Luberto C, Argraves KM. Enzymes of sphingolipid metabolism: from modular to integrative signaling. Biochemistry 2001;40:4893–903.
(19) Colell A, Morales A, Fernandez-Checa JC, Garcia-Ruiz C. Ceramide generated by acidic sphingomyelinase contributes to tumor necrosis factor-alpha-mediated apoptosis in human colon HT-29 cells through glycosphingolipids formation. Possible role of ganglioside GD3. FEBS Lett 2002;526:135–41.
(20) Garcia-Ruiz C, Colell A, Mari M, Morales A, Fernandez-Checa JC. Direct effect of ceramide on the mitochondrial electron transport chain leads to generation of reactive oxygen species. J Biol Chem 1997;272:11369–77.
(21) De Maria R, Lenti L, Malisan F, d'Agostino F, Tomassini B, Zeuner A, et al. Requirement for GD3 ganglioside in CD95- and ceramide-induced apoptosis. Science 1997;277:1652–5.
(22) Andrieu-Abadie N, Levade T. Sphingomyelin hydrolysis during apoptosis. Biochim Biophys Acta 2002;1585:126–34.
(23) Gulbins E, Grassme H. Ceramide and death receptor clustering. Biochim Biophys Acta 2002;1585:139–45.
(24) Zhao H, Miller M, Pfeiffer K, Buras JA, Stahl GL. Anoxia and reoxygenation of human endothelial cells decrease ceramide glucosyltransferase expression and activates caspases. FASEB J 2003;17:723–4.
(25) Biedler JL, Helsan L, Spengler BA. Morphology and growth, tumorigenicity and cytogenetics of human neuroblastoma cells in continuous culture. Cancer Res 1973;33:2643–52.
(26) Jackson AL, Bartz SR, Schelter J, Kobayashi SV, Burchard J, Mao M, et al. Expression profiling reveals off-target gene regulation by RNAi. Nat Biotechnol 2003;21:635–7.
(27) Altschul SF, Gish W, Miller W, Myers EW, Lipman DJ. Basic local alignment search tool. J Mol Biol 1990;215:403–10.
(28) Wiegmann K, Schutze S, Machleidt T, Witte D, Kronke M. Functional dichotomy of neutral and acidic sphingomyelinases in tumor necrosis factor signaling. Cell 1994;78:1005–15.
(29) Di Sano F, Fazi B, Citro G, Lovat PE, Cesareni G, Piacentini M. Glucosylceramide synthase and its funtional interaction with RTN-1C regulate chemotherapeutic drug-induced apoptosis of neuroepithelioma cells. Cancer Res 2003;63:3860–5.
(30) Spinedi A, Di Bartolomeo S, Piacentini M. Apoptosis induced by N-hexanolsphingosine in CHP-100 cells associates with accumulation of endogenous ceramide and is potentiated by inhibition of glucocerebroside synthesis. Cell Death Differ 1998;5:785–91.
(31) Desai K, Sullards C, Allegood J, Wang E, Schmelz EM, Hartl M, et al. Fumonisins and fumonisin analogs as inhibitors of ceramide synthase and inducers of apoptosis. Biochim Biophys Acta 2002;1585:188–92.
(32) Rosner H. Significance of gangliosides in neuronal differentiation of neuroblastoma cells and neurite growth in tissue culture. Ann N Y Acad Sci 1998;845:200–14.
(33) Herget T, Esdar C, Oehrlein S, Heinrich M, Schutze S, Maelicke A, et al. Production of ceramides causes apoptosis during early neuronal differentiation in vitro. J Biol Chem 2000;275:30344–54.
(34) Brann AB, Tcherpakov M, Williams IM, Futerman A, Fainziber M. Nerve growth factor-induced p75-mediated death of cultured hippocampal neurons is age dependent and transduced through ceramide generated by neutral sphingomyelinase. J Biol Chem 2002;277:9812–8.
(35) Copani A, Melchiorri D, Caricasole A, Martini F, Sale P, Carnevale R, et al. Beta-amyloid-induced synthesis of the ganglioside GD3 is a requisite for cell cycle reactivation and apoptosis in neurons. J Neurosci 2002;22:3963–8.
(36) Malisan F, Testi R. GD3 ganglioside and apoptosis. Biochim Biophys Acta 2002;1585:179–87.
(37) Bhunia AK, Schwarzmann G, Chatterjee S. GD3 recruits reactive oxygen species to induce cell proliferation and apoptosis in human aortic smooth muscle cells. J Biol Chem 2002;227:16396–402.
(38) Triche TJ. Neuroblastoma and other childhood neural tumors: a review. Pediatr Pathol 1990;10:175–93.
(39) Bezuglov VV, Fomina-Ageeva EV, Gretskaia NM, Kriukova EV, Diatlovitskaia EV, Bergel'son LD. [Gangliosides modulate lipoxygenase oxidation in human lymphocytes]. Biokhimiia 1991;56:267–72.
(40) DiPietrantonio AM, Hsieh TC, Olson SC, Wu JM. Regulation of G1/S transition and induction of apoptosis in HL-60 leukemia cells by fenretinide (4HPR). Int J Cancer 1998;78:53–61.
(41) Murate T, Suzuki M, Hattori M, Takagi A, Kojima T, Tanizawa T, et al. Up-regulation of acid sphingomyelinase during retinoic acid-induced myeloid differentiation of NB4, a human acute promyelocytic leukemia cell line. J Biol Chem 2002;277:9936–43.
(42) Wiegmann K, Schwandner R, Krut O, Yeh WC, Mak TW, Kronke M. Requirement of FADD for tumor necrosis factor-induced activation of acid sphingomyelinase. J Biol Chem 1999;274:5267–70.
(43) Pettus BJ, Chalfant CE, Hannun YA. Ceramide in apoptosis: an overview and current perspectives. Biochim Biophys Acta 2002;1585:114–25.
(44) Komori H, Ichikawa S, Hirabayashi Y, Ito M. Regulation of UDP-glucose: ceramide glucosyltransferase-1 by ceramide. FEBS Lett 2000;475:247–50.
(45) Komori H, Ichikawa S, Hirabayashi Y, Ito M. Regulation of intracellular ceramide content in B16 melanoma cells. Biological implications of ceramide glycosylation. J Biol Chem 1999;274:8981–7.
(46) Boldin SA, Futerman AH. Up-regulation of glucosylceramide synthesis upon stimulation of axonal growth by basic fibroblast growth factor. Evidence for post-translational modification of glucosylceramide synthase. J Biol Chem 2000;275:9905–9.
(47) Sietsma H, Dijkhuis AJ, Kamps W, Kok JW. Sphingolipids in neuroblastoma: their role in drug resistance mechanisms. Neurochem Res 2002;27:665–74.
(48) Bleicher RJ, Cabot MC. Glucosylceramide synthase and apoptosis. Biochim Biophys Acta 2002;1585:172–8.
(49) Di Sano F, Di Bartolomeo S, Fazi B, Fiorentini C, Matarrese P, Spinedi A, et al. Antisense to glucosylceramide synthase in human neuroepithelioma affects cell growth but not apoptosis. Cell Death Differ 2002; 9:693–5.

NOTES

P. E. Lovat, F. Di Sano, and M. Corazzari contributed equally to this work.

Supported by funding from Cancer and Leukemia in Childhood in the United Kingdom and by Associazione Italiana per la Ricerca sul Cancro, Fondo per gli Investimenti della Ricerca di Base, and Ricerca Corrente e Finalizza, Ministero della Salute in Italy. F. Di Sano and B. Fazi were supported by fellowships from Fondazione Italiana per la Ricerca sul Cancro.

We thank Prof. Dr. Konrad Sandhoff, Kekule-Institut f. Organische Chemie und Biochemie, Bonn, Germany, for the ASMase antibody, and Dr. Holger Lode, Charite Children's Hospital, Humboldt University, Berlin, Germany, for the GD2 antibody.

Manuscript received December 24, 2003; revised June 29, 2004; accepted July 8, 2004.